Supplementary Information

Deposition of Pd/graphene aerogel on nickel foam as a binder free electrode for direct electrooxidation of methanol and ethanol

Chi-Him A. Tsang[a], K.N. Hui[*b], K.S. Hui[*c] and L. Ren[d]

[a] Department of System Engineering and Engineering Management, City University of Hong Kong, Hong Kong

[b] School of Materials Science and Engineering, Pusan National University, San 30 Jangjeon-dong, Geumjeong-gu, Busan 609-735, Republic of Korea

[c] Department of Mechanical Convergence Engineering, Hanyang University, 17 Haengdang-dong, Seongdong-gu, Seoul 133-791, Republic of Korea.

[d] Faculty of Materials and Optoelectronic physics, Xiangtan University, Hunan 411105, P. R. China

[*]Corresponding author

Email addresses: bizhui@pusan.ac.kr (K.N. Hui)

Tel: + 82 5-1510-2467; Fax: + 82 5-1514-4457

E-mail: kshui@hanyang.ac.kr (K.S. Hui)

Tel: +82 2-2220-0441; Fax: +82 2-2220-2299

Figure captions

Fig S1. Digital image of (a) front, and (b) back of the 7.65 wt.% Pd/GA/NF, and optical microscope image of the 7.65 wt.% Pd/GA/NF and the NF, (c-d) low magnification (scale bar: 1000 μm), and (e-f) high magnification (scale bar: 400 μm).

Fig S2. (a-c) TEM images of 0.8 wt.% Pd/GA/NF in 3 random areas (scale bar: (a) and (b): 100 nm, (c): 200 nm), and (d) size distributions of Pd NPs.

Fig S3. (a-c) TEM images of 2.17 wt.% Pd/GA/NF in 3 random areas (scale bar: (a) and (b): 200 nm, (c): 0.5 μm), and (d) size distributions of Pd NPs.

Fig S4. (a-c) TEM images of 7.65 wt.% Pd/GA/NF in 3 random areas (scale bar: 200 nm), and (d) size distributions of Pd NPs.

Fig S5. CV of 2.17 wt.% Pd/GA/NF in 1 M EtOH/1 M KOH (-0.845 to +0.955 V).

Fig S6. The 25^{th} cycle of CV in 1 M MeOH/1 M KOH (-0.245 to +0.955 V) of (a) NF, GA/NF and 7.65 wt.% Pd/GA/NF, and (b) NF; the 25^{th} cycle of CV in 1 M EtOH/1 M KOH (-0.845 to +0.955 V) of (c) NF, GA/NF and 7.65 wt.% Pd/GA/NF, and (d) NF.

Fig S7. CV of 7.65 wt.% Pd/GA/NF in 1 M KOH solution at the 11^{th} cycle (scan rate: 0.05 V s^{-1}).

Table captions

Table S1. Variation of anodic scan J_f, I_f/I_b and onset potential of 7.65 wt.% Pd/GA/NF in methanol oxidation.

Table S2. Variation of anodic scan J_f, I_f/I_b and onset potential of 7.65 wt.% Pd/GA/NF in ethanol oxidation.

Table S3. Comparison of the best values of current density in the anodic scan (J_f) and I_f/I_b ratio of some Pd based electrocatalyst for methanol and ethanol oxidation.

Figures:

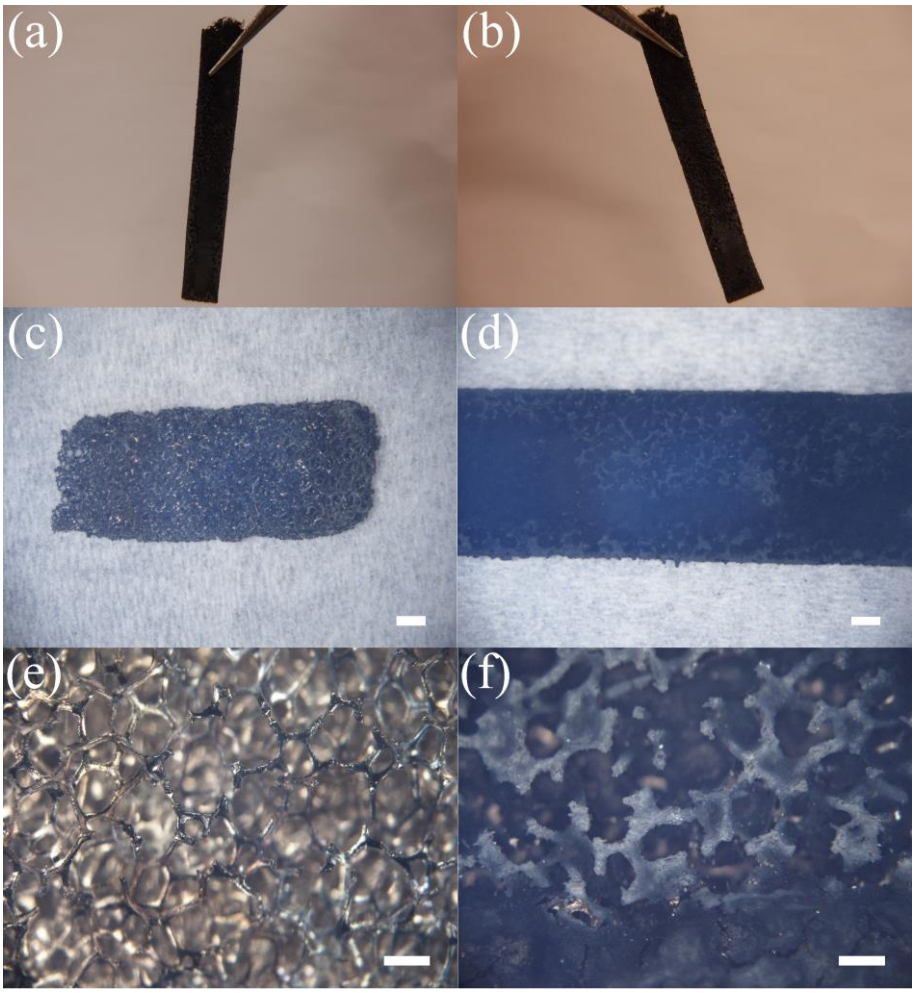

Fig. S1. Digital image of (a) front, and (b) back of the 7.65 wt.% Pd/GA/NF, and optical microscope image of the 7.65 wt.% Pd/GA/NF and the NF, (c-d) low magnification (scale bar: 1000 μm), and (e-f) high magnification (scale bar: 400 μm).

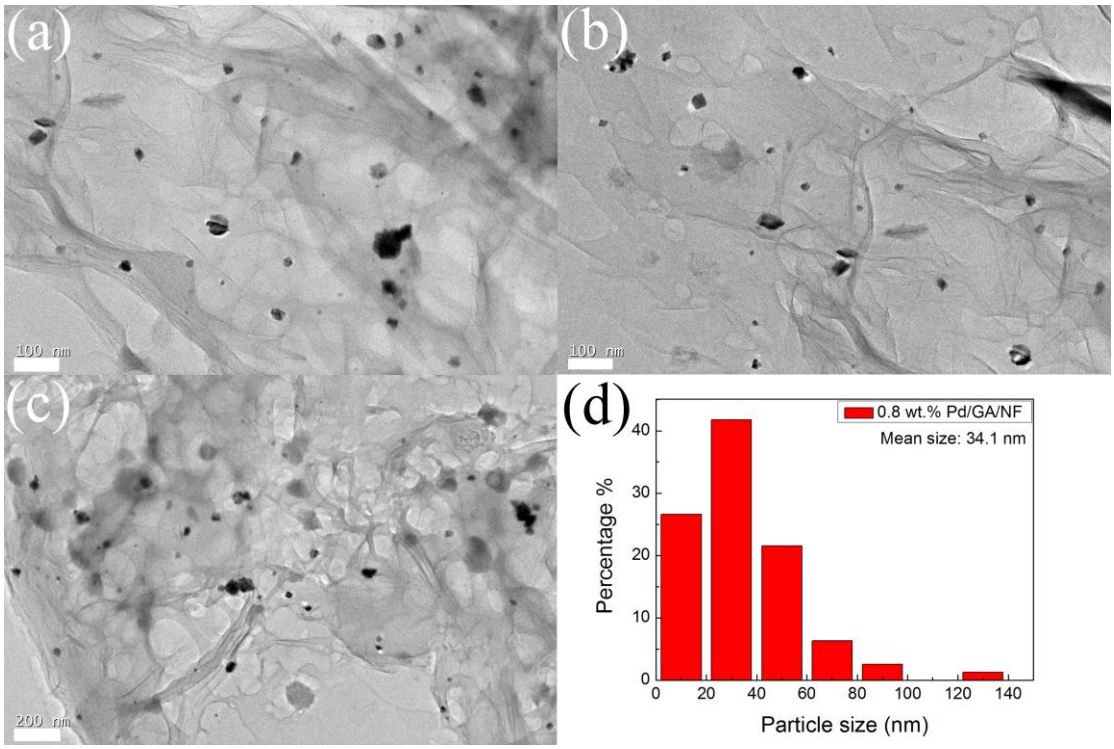

Fig. S2. (a-c) TEM images of 0.8 wt.% Pd/GA/NF in 3 random areas (scale bar: (a) and (b): 100 nm, (c): 200 nm), and (d) size distributions of Pd NPs.

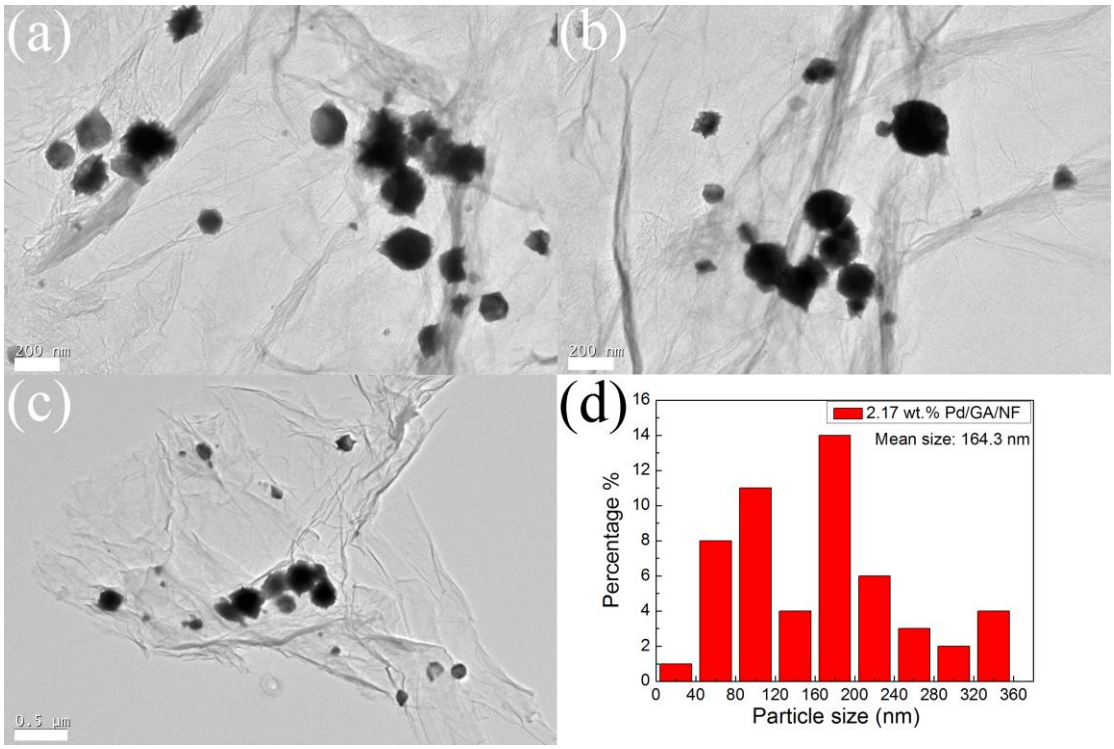

Fig. S3. (a-c) TEM images of 2.17 wt.% Pd/GA/NF in 3 random areas (scale bar: (a) and (b): 200 nm, (c): 0.5 µm), and (d) size distributions of Pd NPs.

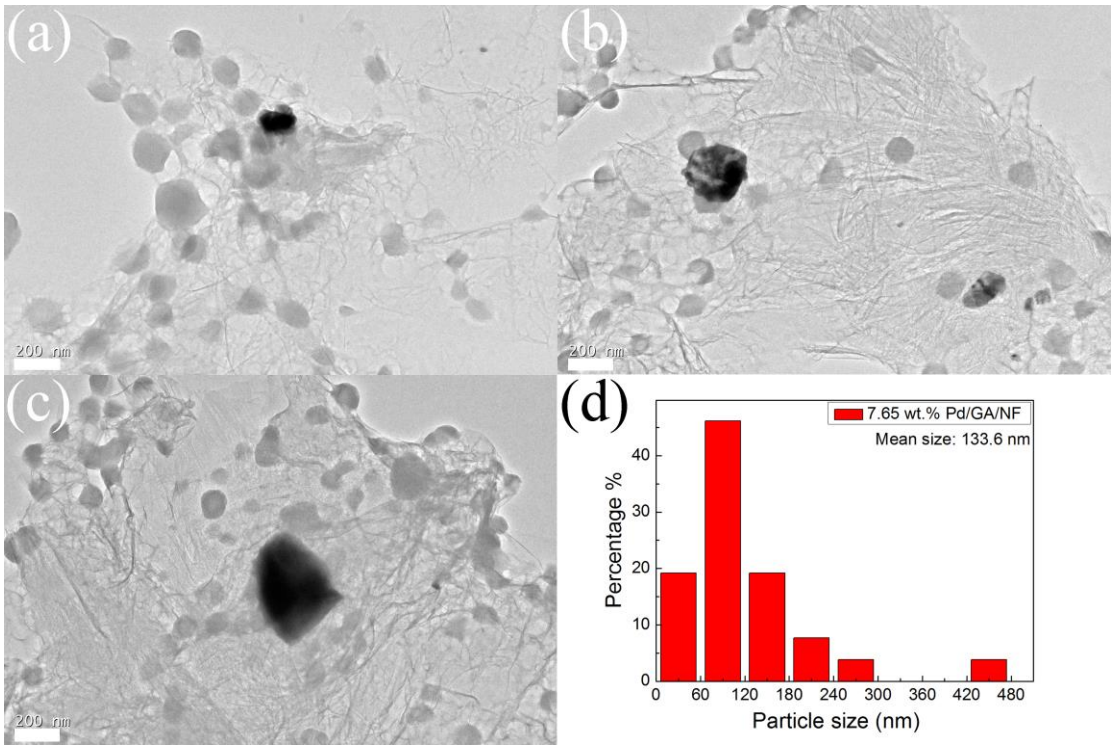

Fig. S4. (a-c) TEM images of 7.65 wt.% Pd/GA/NF in 3 random areas (scale bar: 200 nm), and (d) size distributions of Pd NPs.

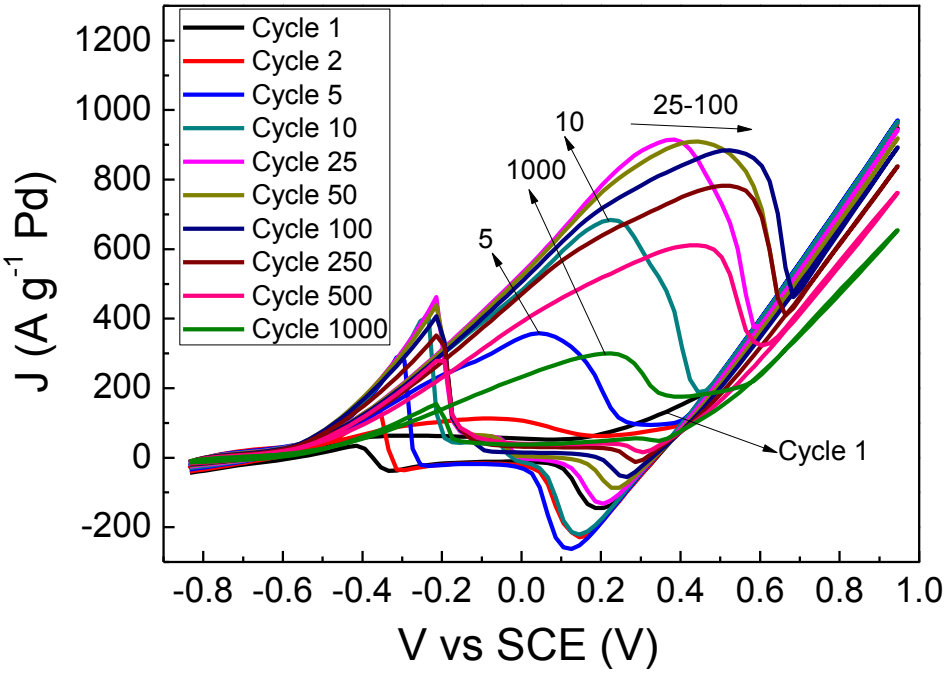

Fig. S5. CV of 2.17 wt.% Pd/GA/NF in 1 M EtOH/1 M KOH (-0.845 to +0.955 V).

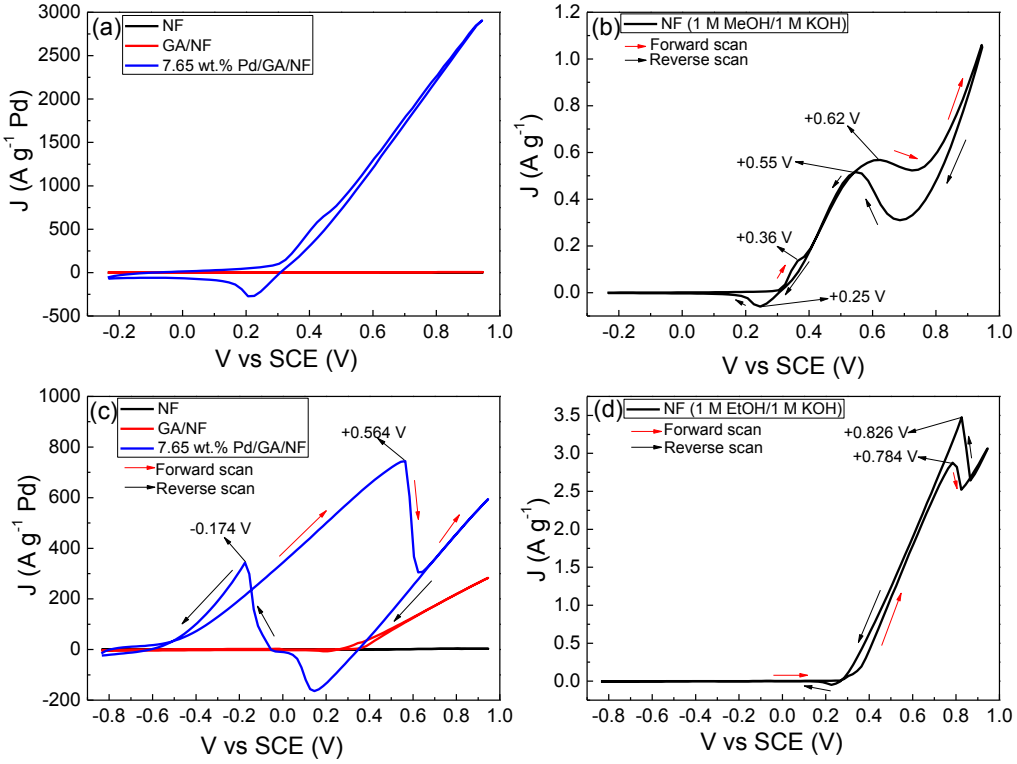

Fig. S6. The 25th cycle of CV in 1 M MeOH/1 M KOH (-0.245 to +0.955 V) of (a) NF, GA/NF and 7.65 wt.% Pd/GA/NF, and (b) NF; the 25th cycle of CV in 1 M EtOH/1 M KOH (-0.845 to +0.955 V) of (c) NF, GA/NF and 7.65 wt.% Pd/GA/NF, and (d) NF.

CV behavior of 7.65 wt.% Pd/GA/NF in 1 M KOH

In-depth analysis of electrocatalytic performance of 7.65 wt.% Pd/GA/NF was performed. Fig. S7 shows the CV curve of 7.65 wt.% Pd/GA/NF in 1 M KOH solution at the 11th cycle at 25 ^{o}C. The result indicated an obvious cathodic peak at -0.43 V in the reverse scan, which was due to oxygen desorption from the Pd NPs in alkaline solution.[1]

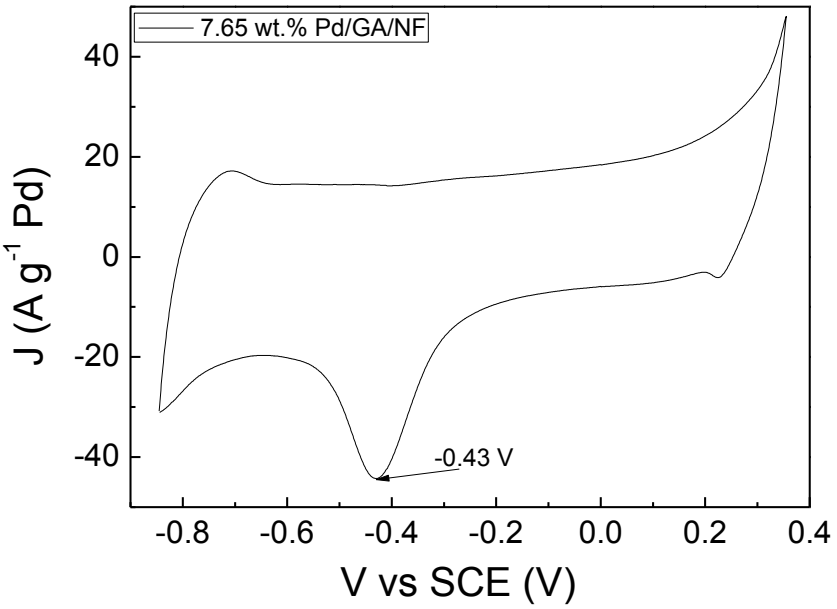

Fig. S7. C CV of 7.65 wt.% Pd/GA/NF in 1 M KOH solution at the 11th cycle (scan rate: 0.05 V s^{-1}).

Table S1 Variation of anodic scan J_f, I_f/I_b and onset potential of 7.65 wt.% Pd/GA/NF in methanol oxidation.

Cycle number	J_f (A g^{-1}) (MeOH)	I_f/I_b (MeOH)	Variation rate of J_f (MeOH)	Onset potential (V) (MeOH)
1	593.3	4.15	0.74	-0.476
5	715.2	3.46	0.90	-0.476
6	733.2	2.86	0.92	-0.476
9	755.8	3.51	0.95	-0.496
14	798.8	3.11	1	-0.496
25	787.97	3.03	0.99	-0.496
29	788	3.05	0.99	-0.536
54	729.9	2.96	0.91	-0.516
104	670.2	3.03	0.84	-0.516
254	590	2.70	0.74	-0.516
504	492.4	2.09	0.62	-0.516
1004	316	1.61	0.40	-0.496

Table S2 Variation of anodic scan J_f, I_f/I_b and onset potential of 7.65 wt.% Pd/GA/NF in ethanol oxidation.

Cycle number	J_f (A g^{-1}) (EtOH)	I_f/I_b (EtOH)	Variation rate of J_f (EtOH)	Onset potential (V) (EtOH)
1	60.5	0.52	0.07	-0.436
5	288.3	1.35	0.33	-0.536
25	744.3	2.17	0.85	-0.596
31	786	2.22	0.90	-0.616
32	792	2.24	0.91	-0.616
35	801	2.29	0.92	-0.596
40	807	2.28	0.92	-0.616
55	819.3	2.32	0.94	-0.616
80	827	2.36	0.95	-0.596
130	835	2.54	0.96	-0.616
280	874	2.72	1	-0.616
530	862	2.89	0.99	-0.636
1004	606.86	2.15	0.69	-0.616
1030	590.2	2.13	0.68	-0.616

Table S3 Comparison of the best values of current density in the anodic scan (J_f) and I_f/I_b ratio of some Pd based electrocatalyst for methanol and ethanol oxidation.

Catalyst	J_f (MeOH/KOH)	J_f (EtOH/KOH)	I_f/I_b (MeOH)	I_f/I_b (EtOH)	Reference electrode	Ref
LDG/Pd	27.6 (mA cm^{-2})	N/A	N/A	N/A	Hg/HgO	[1]
Porous Pd	238 (A g^{-1} Pd)	N/A	N/A	N/A	Hg/HgO	[2]
Pd/CNT	274.5 (A g^{-1} Pd)	135 (A g^{-1} Pd)	<1	<1	Hg/HgO	[3]
Pd/graphene	N/A	0.56 (mA cm^{-2})	N/A	4.0	Ag/AgCl	[4]
Pd/graphene	522 (A g^{-1} Pd)	N/A	6.05	N/A	SCE	[5]
Pd/C	N/A	102.8 (A g^{-1})	N/A	0.7	Hg/HgO	[6]
Pd/C	N/A	114 (mA cm^{-2})	N/A	N/A	Hg/HgO	[7]
Pd-F/CNT	32.7 (mA cm^{-2})	N/A	3.13	N/A	SCE	[8]
Pd/LDH-NWs	N/A	2.01 (mA cm^{-2})	N/A	0.91	Hg/HgO	[9]
Pd nanocubes	15.6 (A g^{-1})	18.72 (A g^{-1})	2	<1	NHE	[10]
0.8 wt.% Pd/GA/NF	N/A	394.7 (A g^{-1} Pd)	N/A	2.66	SCE	This work
2.17 wt.% Pd/GA/NF	187.3 (A g^{-1} Pd)	914.7 (A g^{-1} Pd)	2.58	1.97	SCE	This work
7.65 wt.% Pd/GA/NF	798.8 (A g^{-1} Pd)	874 (A g^{-1} Pd)	3.11	2.72	SCE	This work

References:

1. H. J. Huang and X. Wang, *J. Mater. Chem.*, 2012, **22**, 22533-22541.
2. R. S. Li, H. Mao, J. J. Zhang, T. Huang and A. S. Yu, *J. Power Sources*, 2013, **241**, 660-667.
3. F. C. Zhu, G. S. Ma, Z. C. Bai, R. Q. Hang, B. Tang, Z. H. Zhang and X. G. Wang, *J. Power Sources*, 2013, **242**, 610-620.
4. X. Yang, Q. D. Yang, J. Xu and C. S. Lee, *J. Mater. Chem.*, 2012, **22**, 8057-8062.
5. Y. Wang, Y. Zhao, W. T. He, J. Yin and Y. Q. Su, *Thin Solid Films*, 2013, **544**, 88-92.
6. S. Y. Shen and T. S. Zhao, *J. Mater. Chem. A*, 2013, **1**, 906-912.
7. S. Y. Shen, T. S. Zhao, J. B. Xu and Y. S. Li, *J. Power Sources*, 2010, **195**, 1001-1006.
8. X. L. Yang, M. M. Zhen, G. Li, X. Z. Liu, X. Y. Wang, C. Y. Shu, L. Jiang and C. R. Wang, *J. Mater. Chem. A*, 2013, **1**, 8105-8110.
9. J. W. Zhao, M. F. Shao, D. P. Yan, S. T. Zhang, Z. Z. Lu, Z. X. Li, X. Z. Cao, B. Y. Wang, M. Wei, D. G. Evans and X. Duan, *J. Mater. Chem. A*, 2013, **1**, 5840-5846.
10. N. Arjona, M. Guerra-Balcazar, L. Ortiz-Frade, G. Osorio-Monreal, L. Alvarez-Contreras, J. Ledesma-Garcia and L. G. Arriaga, *J. Mater. Chem. A*, 2013, **1**, 15524-15529.